TÜBİTAK

Turk J Phys
33 (2009) , 281 – 298.

doi:10.3906/fiz-0901-7

Heavy ion reactions producing a heavier deformed nucleus and free nucleons

Ahmed OSMAN
Physics Department, Faculty of Science, Cairo University, Cairo-EGYPT
ahmedosman_1944@yahoo.com

Received 16.01.2009

Abstract

Carbon induced heavy ion reactions on the heavy ^{197}Au target are considered. The statistical scission model is used to calculate this fission process. In the present considered reactions, the process leads to the fragmentation of only one deformed heavy fragment and few nucleons. Angular distributions of the fission fragments are numerically calculated for different values of the incident energies in the range 64–104 MeV. The present theoretical calculations of the differential cross-sections are in good agreements with experimental data for the carbon incident energy 84 A MeV. The effective variance of this fission process is also calculated. The present numerically calculated values of the variance and angular distributions are in good agreement with previously calculated values.

Key Words: Fission reactions, charged particle induced fission, mulifragmentation, ^{12}C + ^{197}Au reactions, calculated angular distributions and variances.

The PACS Subject Index Categories: 25.85.Ge, 25.70.Np, 25.70.Jj.

1. Introduction

The statistical transition state model (TSM) [1] provides a good representation of the fragment angular distributions from low energy nuclei fission with finite barriers and well defined transition state configurations. The saddle point in the potential energy surface for nuclear shape degrees of freedom in this model represents a distinct point in the fission trajectory where the direction of the fission axis with respect to the nuclear spin I is determined. Also assumed in the TSM model is that the spin projection K on the nuclear symmetry axis remains unchanged during the subsequent descent from the saddle to the scission point. The TSM model is extended [2–8] to the domain of fusion-like heavy ion reactions by a small modification [9] to include the dependence of the transition state shape on the quantum number K, which leads to a minor change in the theoretical angular distributions for most reactions. The breakdown of the fundamental assumption of the

TSM model for heavy nuclei requires a rather different approach to describe the fission of heavy systems. The various directions of the fission axis of an axially symmetric nucleus according to this theory are assumed to be populated due to the density of the intrinsic transitions states, depending on the moments of inertia of the nucleus for collective rotations about its principle axes and also on the nuclear temperature. The moments of inertia are related to the spin-dependent saddle point shapes which are axially symmetric for lighter systems, and triaxial for heavy nuclei as predicted from the rotating liquid drop model [10] RLDM.

The transition state theory is inapplicable for nuclear spins in excess of the RLDM stability limit, since an equilibrium point in the potential energy no longer exists. This inapplicability may occur also when the nuclear temperature exceeds magnitudes equivalent to the height of the fission barrier [8].

The statistical scission model SSM has been suggested [11] for heavy ion reactions with small or negligible fission barriers by assuming a statistical fractionation of the total angular momentum among all angular momentum carrying degrees of freedom of the two separated fission fragments. SSM is applicable for very small values of the fission barriers and when the angular momentum and excitation energy are very large. It introduces definite predictions of the angular distributions, based on the level densities associated with a unique final fragment configuration.

In the present work, we introduce a study for heavy ion reactions producing a heavier deformed nucleus and free nucleons. The theory of these reactions is developed following the statistical scission model. In the present work, we consider the heavy ion reaction $^{12}\mathrm{C} + {}^{197}\mathrm{Au}$ leading to three different exit channels. The first case is that of outgoing particles as $^{205}\mathrm{Tl} + 4\ {}^{1}\mathrm{P}_{1}$, while the second is that leading to $^{206}\mathrm{Pb} + 3\ {}^{1}\mathrm{P}_{1}$ and the third one result to the products of $^{202}\mathrm{Hg} + 5\ {}^{1}\mathrm{P}_{1} + 2\ {}^{1}\mathrm{n}_{0}$. Numerical calculations of the angular distributions of each case of heavy ion reaction are carried out at different values of the incident energies. The common feature of all three reactions is that the exit channels are a deformed nucleus and few light particles.

The formalism of multifragmentation theory is introduced in section 2, following the statistical scission model. Numerical calculations and results are presented in section 3. Discussion and conclusions are given in scission 4.

2. Multifragmentation formalism

The relative cross section for the emitted fission fragments depends on the transmission coefficients, the fission probability for a state in the composite nucleus and on the normalized rigid rotor functions. These quantities are denoted by $T_l\Gamma_f(E,I,m)/\Gamma(E,I)$ and $D^I_{M,m}(\theta)$, respectively, where E is the excitation energy of the composite nucleus and I is its spin with projection m. The quantity $\Gamma(E,I)$ represents the total decay of the states. The ratio $T_l\Gamma_f(E,I,m)/\Gamma(E,I)$ can be written as

$$[\Gamma_f(E,I,m)/\Gamma_f(E,I)]\ \ [\Gamma_f(E,I)/\Gamma(E,I)] \tag{1}$$

Systems with finite evaporation residue cross sections are considered on the assumption that these cross sections deplete the smaller values of I up to I_{min}. In our calculations the ratio $\Gamma_f(E,I)/\Gamma(E,I)$ is assumed to be unity for a range of angular momenta values $I_{min} > I \geq I_{max}$, and zero otherwise. For the case that the target and projectile spins as well as the spin projection are zero, the relative cross section is given by the expression

as

$$W(E,\theta) \propto \sum_{I,m} (2I+1)T_I \ \ [\Gamma_f(E,I,m)/\Gamma(E,I)] \cdot (I+1/2) \left| D^I_{M=\theta,m}\ (\theta) \right|^2 \tag{2}$$

with

$$\Gamma_f(E,I) = \sum_m \Gamma_f(E,I,m)$$

In equation (2), the relative fission decay width $\Gamma_f(E,I,m)$ is written as the product of the inverse cross section and the density of the final states, considering the fission as a process of complex particle evaporation. Therefore

$$\Gamma_f(E,I,m) \propto \sum_{\ell,s} (2\ell+1) exp[-\ell^2\hbar^2/2T\mu R_\circ^2] \cdot \left| \langle Sm\ell\ 0 |\, Im\rangle \right|^2 \rho\ (E,S,m). \tag{3}$$

The orbital angular momentum ℓ in the exit channel is perpendicular to the fission axis. The channel spin S is the vector sum of the two fission fragment spins as $\mathbf{s} = \mathbf{i}_1 + \mathbf{i}_2$. The total energy available at the scission configuration for the case $\ell = 0$ is given by the expression

$$E = E_{cm} + Q_{FF} - E_K - E_D - E_{PS}, \tag{4}$$

where E_{cm} is the center of mass energy in the entrance channel, Q_{FF} is the Q value of the fission reaction, E_K is the total kinetic energy of the fission fragments (FF) for $\ell = 0$, E_D is the deformation energy of the fission fragments, and E_{PS} is the energy associated with precession (PS) particle emission. The total excitation energy of the two fragments, including their thermal and intrinsic rotational energies, is $E - E_R(\ell)$, where the orbital rotational energy E_R for angular momentum ℓ is given by the function $E_R(\ell) = \ell^2\hbar^2/2\mu R_C^2$. μ is the reduced mass of the fission channel while R_C is the distance between the centers of the fission fragments at the scission configuration. In equation (3), the product $\rho(E,S,m)exp[-E_R(\ell)/T]$ represents the intrinsic level density of the two fission fragments in the constant temperature level-density formalism. In case of a fixed value for the total angular momentum $\mathbf{I}$, the probability of any given set values $\mathbf{S}$, $\mathbf{m}$ and ℓ is determined by the available thermal excitation energy [12]. Density of states at scission can be calculated using the density of states of the two fission fragments, (for uncorrelated fragment spins $\mathbf{i}_1$ and $\mathbf{i}_2$), the total spin $\mathbf{S}$ and its projection $\mathbf{m}$ on the fission direction, which can be given semi-classically [11] by the expression

$$\rho(E,S,m) \approx \iiint \rho_1(E_1^*,i_1)\rho_2(E_2^*,i_2)\delta^3(E_1^* + E_2^* - E_3)dE_1^*dE_2^*dE_3^*d^3i_1d^3i_2 \tag{5}$$

Here, E is the excitation energy at scission and is given by the sum of the excitation energies E_1^* and E_2^* of the two fragments.

Also, the channel spin $\mathrm{S} = \mathrm{i}_1 + \mathrm{i}_2$ couples with the orbital angular momentum ℓ giving the total spin I.

Spherical fission fragments

In case of fission process with spherical fragments, the quantities $\rho_\gamma(E_\gamma)$ presented in equation (5) can be replaced by their mean values as

$$\rho_1(\langle E_1^*\rangle) = \rho_2(\langle E_2^*\rangle) = \rho(\langle E/2\rangle),$$

where the spin cutoff parameters of the fragments are taken to be equal $\sigma_1^2 = \sigma_2^2 = \sigma^2$. The excitation energies of the fission fragments at scission configuration depend on the orbital angular momentum ℓ due to the collective rotation of the system with influence on the density of states expressed by the factor $\exp(-\ell^2\hbar^2/2T_\mu R_C^2)$ in equation (3). If the total excitation energy E_γ^* of a nucleus is large enough relative to its rotational energy E_R, then the density of states for one of the fragments can be approximated by the product of energy and spin dependent terms as

$$\begin{aligned} \rho(E_\gamma^*, i_\gamma) &\approx \rho[E_\gamma^* - E_R(i_\gamma), 0] \\ &\propto \rho(E_\gamma^*) exp[-(i_\gamma + 1/2)^2/2\sigma^2]. \end{aligned} \tag{6}$$

Also, the integrals of the spin-dependent part of the state density in equation (5) can be expressed as sum over i_γ and m_γ as

$$\begin{aligned} \int \rho(i_\gamma) d^3 i_\gamma &\propto \int exp[-(i_\gamma + 1/2)^2/2\sigma_\gamma^2] i_\gamma^2 di_\gamma d\Omega_\gamma \\ &\propto \sum_{i_\gamma m_\gamma} (2i_\gamma + 1) exp[-(i_\gamma + 1/2)^2/2\sigma_\gamma^2]. \end{aligned} \tag{7}$$

Therefore, equation (5) becomes

$$\begin{aligned} \rho(S, m) \propto \sum_{i_1 m_1 i_2 m_2} |\langle\, i_1 m_1 i_2 m_2 \,|Sm\,\rangle|^2 \quad &\cdot(2i_1 + 1) exp[-(i_1 + 1/2)^2/2\sigma^2] \\ &\cdot(2i_2 + 1) exp[-(i_2 + 1/2)^2/2\sigma^2]. \end{aligned} \tag{8}$$

After performing the summation in equation (8), the form of $\rho(S, m)$ is simplified to the form

$$\rho(S, m) \propto (2S + 1) exp[-(S + 1/2)^2/2(2\sigma^2)]. \tag{9}$$

Introducing equation (9) into equation (3), and performing the sums over orbital angular momentum ℓ and channel spin S, the spin-dependent fission at a fixed excitation energy E is given by

$$\Gamma_f(I, m)/\Gamma_f(I) = exp(-m/2S_0^2)/\sum_{m^\cdot} exp(-m^-)^2/2S_0^2). \tag{10}$$

The variance S_0^2 for spherical fragments is given by

$$S_0^2 = 2\sigma^2\{[2\sigma^2 + (\mu R_C^2 T/\hbar^2)]/\mu R_C^2 T/\hbar^{2)}\},$$

or in the form

$$S_0^2 = (2I_o T/\hbar^2)[(2I_o + \mu R_C^2)/\mu R_C^2], \tag{11}$$

since

$$\sigma^2 = I_o T/\hbar^2 = (2/5) M R^2 T/\hbar^2.$$

The quantities I_o, T, M and R stand for the moment of inertia, nuclear temperature, mass, and radius of one of the symmetric fragments, respectively. Introducing equation (10) into equation (2), the relative cross section for fixed energy E is given by the expression as

$$W(\theta) = \sum_{I_{min}}^{I_{max}} (2I{+}1) T \; \frac{\sum\limits_{m=-I}^{I} [(2I{+}1)/2] \left| D^I_{M=0,m}(\theta) \right|^2 exp(-m^2/2S_0^2)}{\sum\limits_{m=-I}^{I} \exp(-m^2/2S_0^2)}. \tag{12}$$

3. Deformed fission fragments

The emission axis for fission fragments is assumed to coincide, in the case of aligned deformed fragments, so that $k_1 = m_1$ and $k_2 = m_2$.

The density of states for each one of the deformed fragments can be written as

$$\rho\left(E^*, i\right) \propto \rho\left(E^*\right) exp\left[-\left\{(i+1/2)^2/2\sigma_\perp^2\right\} - \left\{m^2/2\sigma_{eff}^2\right\}\right], \tag{13}$$

where m is the projection of the spin **i** on the symmetry axis of the nucleus coinciding with the fission direction. The effective spin cutoff parameter σ_{eff} controls the dependence of the density of states with projection m on the symmetry axis, where

$$\sigma_{eff}^2 = \sigma_{||}^2\sigma_\perp^2/(\sigma_\perp^2 - \sigma_{||}^2). \tag{14}$$

The quantities $\sigma_\perp^2$ and $\sigma_{||}^2$ are related to the corresponding moments of inertia $I_\perp$ and $I_{||}$ of a rigid rotor for the case of rotation about an axis perpendicular or parallel to the symmetry axis, respectively, and to the nuclear temperature T of the nucleus by the relation $\sigma_\perp^2 = I_\perp T/\hbar^2$ and $\sigma_{||}^2 = I_{||}T/\hbar^2$. Also, as has been done in equation (7), the spin-dependent parts of the state density integrals in equation (5) can be expressed as a sum over i and m as

$$\begin{aligned} \int \rho(i) d^3 i \quad &\propto \int \exp\left[-\left\{(i+1/2)^2/2\sigma_\perp^2\right\} - \left\{m^2/2\sigma_{eff}^2\right\}\right] i^2\, did\Omega \\ &\propto \sum_{i,m} (2i+1) \exp\left[-\left\{(i+1/2)^2/2\sigma_\perp^2\right\} - \left\{m^2/2\sigma_{eff}^2\right\}\right]. \end{aligned} \tag{15}$$

Therefore, the density of state for deformed fission fragments with channels spin S and projection m on the fragments emission axis can be written as

$$\rho(S,m) \propto \sum_{i_1\, m_1\, i_2\, m_2} \left\{ \begin{array}{l} \left|\langle i_1\, m_1\, i_2\, m_2 \,|Sm\rangle\right|^2 (2i_1+1) \\ \cdot exp\left[-\left\{(i_1+1/2)^2/2\sigma_\perp^2\right\} - \left\{m_1^2/2\sigma_{eff}^2\right\}\right] \\ \cdot (2i_2+1) exp\left[-\left\{(i_2+1/2)^2/2\sigma_\perp^2\right\} - \left\{m_2^2/2\sigma_{eff}^2\right\}\right] \end{array} \right\}. \tag{16}$$

Equation (16) can be approximated to the form

$$\rho(S,m) \propto (2S+1) \exp\left[-\left\{(S+{}^1/_2)^2/2\chi 2\sigma_\perp^2\right\} - \left\{m^2/2\chi\sigma_{eff}^2\right\}\right]. \tag{17}$$

With this, approximation introduced in equation (3) allows one to calculate the ratio $\Gamma_f(E, I, m)/\Gamma(E, I)$ for fixed value of I and m. The summation over ℓ and S in equation (3) leads to an equation of the same form as equation (10), except that the variance S_0^2 will then have the expressions

$$\begin{aligned} S_0^2 &= 2\sigma_{||}^2\{[2\sigma_\perp^2 + (T\mu R_C^2/\hbar^2)]/(T\mu R_C^2/\hbar^2) + 2\sigma_\perp^2 - 2\sigma_{||}^2\}, \\ S_0^2 &= (2I_{||}T/\hbar^2)[2I_\perp + \mu R_C^2)/(\mu R_C^2 + 2I_\perp - 2I_{||})]. \end{aligned} \tag{18}$$

In equation (18), $\sigma_\perp^2$, $\sigma_{||}^2$, $I_\perp$, $I_{||}$ are the spin cutoff parameters and the moments of inertia for a single fission fragments, rotating about an axis parallel and perpendicular to its symmetry axis (and fission axis), respectively.

4. Numerical calculations and results

In the present work, we study the ^{12}C + ^{197}Au reactions in which three types of reaction products are formed in the exit channel. Each of these types have has in the exit channel only one deformed fission fragment and few protons or few protons and few neutrons. The present considered three types of the reactions in the exit channel are ^{205}pb + 3 ^{1}P , ^{206}T1 + 4 ^{1}P and ^{202}Hg + 5 ^{1}P + 2 ^{1}n with reaction Q-values given as -27.717 MeV, -34.47045 MeV and -53.85127 MeV, respectively. The angular distributions of fission products are calculated by using the statistical scission model. The symmetric top wave functions $\left|D^{I}_{M=0,m}\left(\theta\right)\right|^{2}$ appeared in equation (2) can be written as (13),

$$\left|D^{I}_{M=0,m}\left(\theta\right)\right|^{2} \approx (1/\pi)\left[(I+1/2)^{2}sin^{2}\theta - m^{2}\right]^{-1/2} \tag{19}$$

while the variances S_0^2 may be estimated using the formula

$$S_0^2 = \sum \sigma_i^2, \tag{20}$$

and where the summation is to be done for all fission fragments for each reaction. The spin cut-off factors associated with the level density of each fission fragments is given by [13]

$$\sigma_i^2 = 2/5MR^2T/\hbar^2. \tag{21}$$

M and R are the mass and the radius of each fragment and T is the nuclear temperature [14] expressed as

$$T = \left[8/A(E_{cm} + Q - E_K)\right]^{1/2}. \tag{22}$$

In equation (22), A, E_{cm} and Q are the nucleon number, the center of mass bombarding energy and the Q-value of the reaction channel leading to fission fragments, respectively. E_K is the average summed kinetic energies of the fragments given by

$$E_K = 0.107Z^2/A^{1/3} + 22MeV,$$

where Z and A are the charge and mass numbers of the compound nucleus which are in our case $Z = 209$ and $A = 85$. For the case of deformed fission fragments, we used the relation

$$\chi^{2/3}(\chi^2 - 1)/\chi^2 + 1 = I_{sph}/I_{eff} = (I_{sph}/\hbar^2)(T/K_0^2).$$

Therefore $\sigma^2_{def} = 2/5(I_{eff}T/\hbar^2)$, where we used in the present calculations the value of $\chi = 2$. The incident laboratory energy is taken in the range 64 MeV per nucleon to 104 MeV per nucleon, which means that, in the present case, 768 MeV to 1248 MeV, since the incident particle is ^{12}C. This corresponds to center of mass energy range 722.963 MeV to 11767.333 MeV, the values of which is very high relative to the deformation energy and to the Q-value; so that in the present work, and for this reason, we consider $E_D \approx 0$.

Numerical calculations are carried out for angular distribution cross sections $W(\theta)$, the ratio $W(\theta)/W(90)$ and also for the variances S_0^2 for the three different types of the reaction products. The transmission coefficient T_ℓ in all our calculations for all different cases is taken to be unity.

The obtained results of the present calculations are shown in Figures (1)–(19).

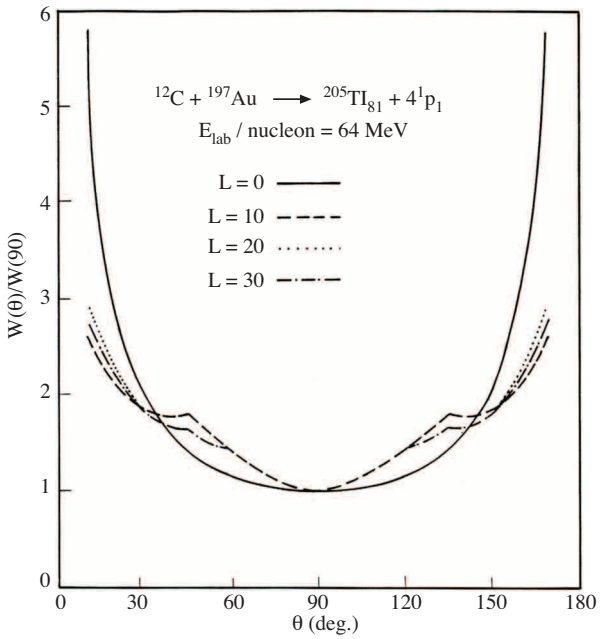

Figure 1. Angular distributions of the fission fragments from the $^{12}C + ^{197}Au \rightarrow ^{205}Tl_{81} + 4\,^{1}P_{1}$ reaction at different values of the angular momentum. The nuclear temperature has a value $T = 4.029$ MeV. The laboratory energy is E_{lab} / nucleon = 64 MeV.

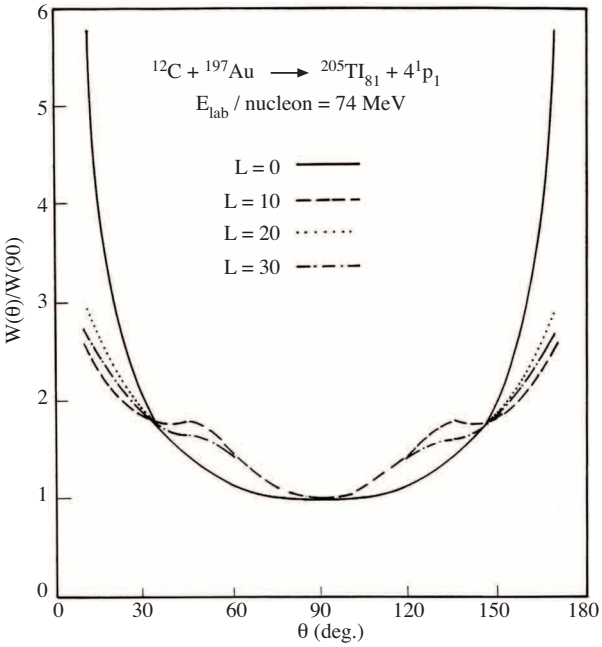

Figure 2. Angular distributions of the fission fragments from the $^{12}C + ^{197}Au \rightarrow ^{205}Tl_{81} + 4\,^{1}P_{1}$ reaction at different values of the angular momentum. The nuclear temperature has a value $T = 4.534$ MeV. The laboratory energy is E_{lab} / nucleon = 74 MeV.

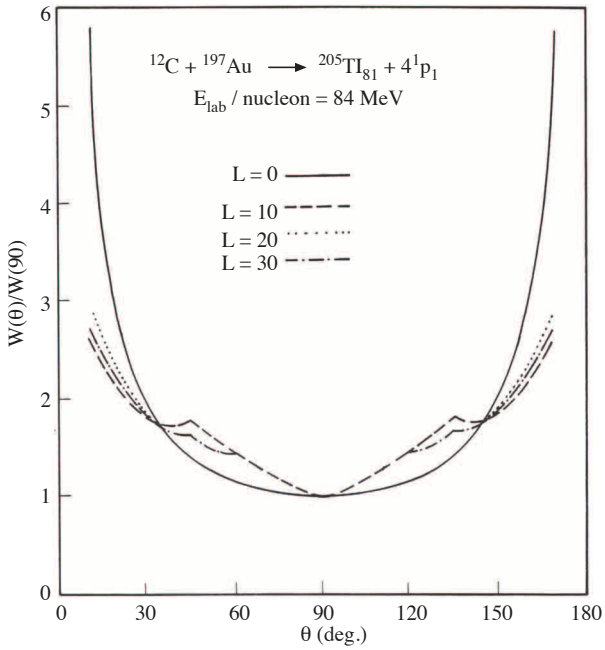

Figure 3. Angular distributions of the fission fragments from the $^{12}\mathrm{C}+\ ^{197}\mathrm{Au}\ \rightarrow^{205}\mathrm{T1}_{81}\ +4\ ^{1}\mathrm{P}_{1}$ reaction at different values of the angular momentum. The nuclear temperature has a value $T\ =4.989$ MeV. The laboratory energy is E_{lab} / nucleon = 84 MeV.

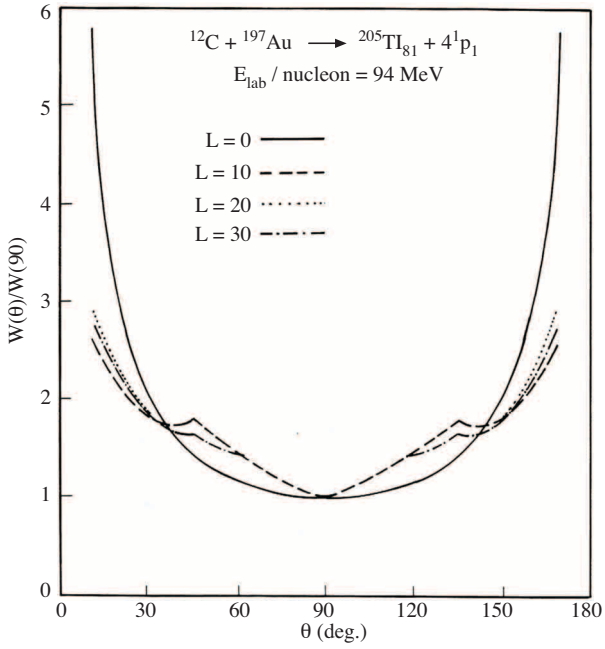

Figure 4. Angular distributions of the fission fragments from the $^{12}\mathrm{C}+\ ^{197}\mathrm{Au}\ \rightarrow^{205}\mathrm{T1}_{81}\ +4\ ^{1}\mathrm{P}_{1}$ reaction at different values of the angular momentum. The nuclear temperature has a value $T\ =5.406$ MeV. The laboratory energy is E_{lab} / nucleon = 94 MeV.

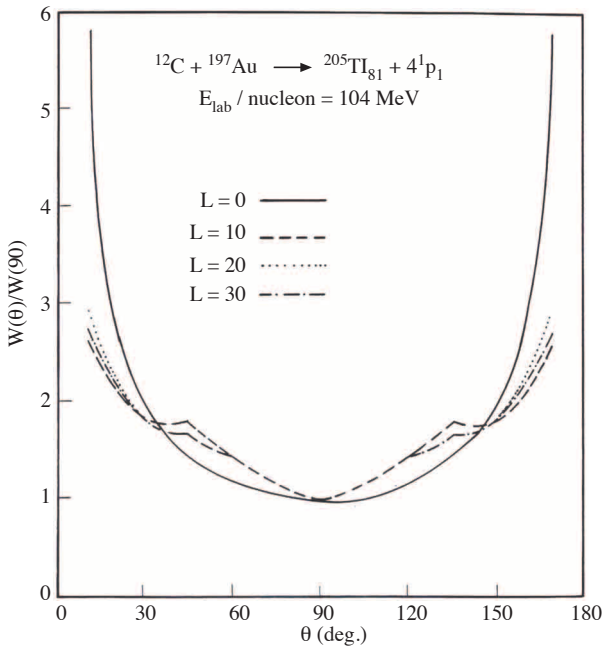

Figure 5. Angular distributions of the fission fragments from the $^{12}C + ^{197}Au \rightarrow ^{205}T1_{81} + 4\ ^1P_1$ reaction at different values of the angular momentum. The nuclear temperature has a value $T = 5.792$ MeV. The laboratory energy is E_{lab} / nucleon = 104 MeV.

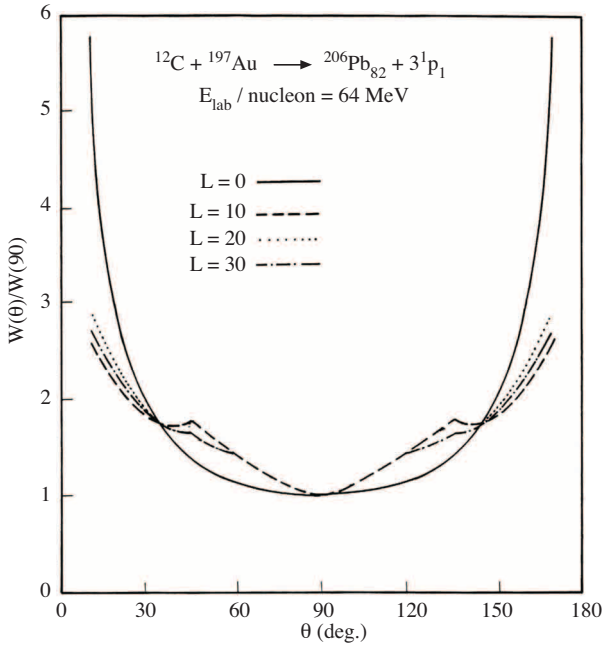

Figure 6. Angular distributions of the fission fragments from the $^{12}C + ^{197}Au \rightarrow ^{206}pb_{82} + 3\ ^1P_1$ reaction at different values of the angular momentum. The nuclear temperature has a value $T = 4.060$ MeV. The laboratory energy is E_{lab} / nucleon = 64 MeV.

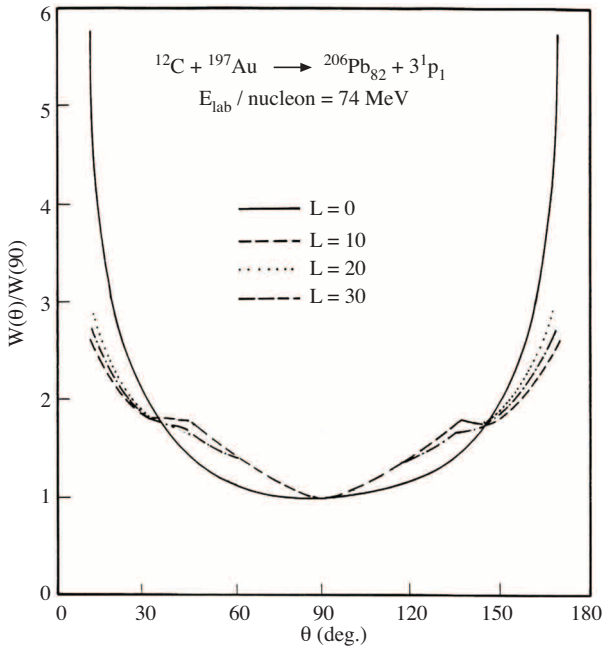

Figure 7. Angular distributions of the fission fragments from the $^{12}\mathrm{C}+\ ^{197}\mathrm{Au} \rightarrow ^{206}\mathrm{pb}_{82} + 3\ ^{1}\mathrm{P}_{1}$ reaction at different values of the angular momentum. The nuclear temperature has a value $T = 4.563$ MeV. The laboratory energy is E_{lab} / nucleon = 74 MeV.

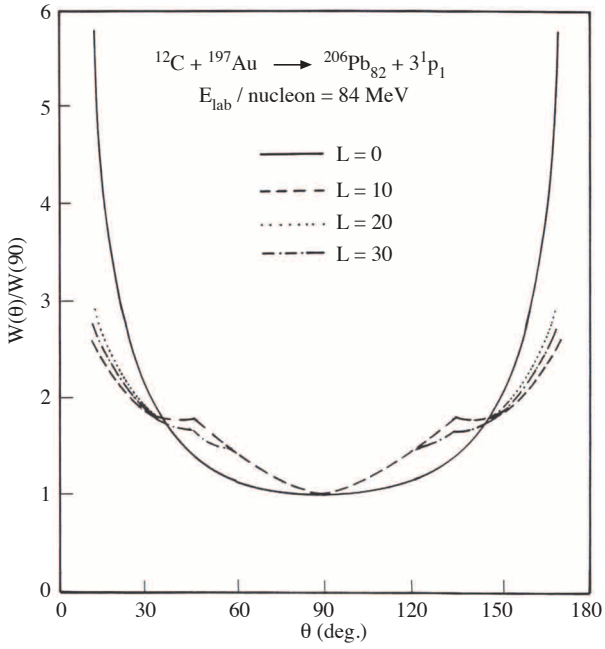

Figure 8. Angular distributions of the fission fragments from the $^{12}\mathrm{C}+\ ^{197}\mathrm{Au} \rightarrow ^{206}\mathrm{pb}_{82} + 3\ ^{1}\mathrm{P}_{1}$ reaction at different values of the angular momentum. The nuclear temperature has a value $T = 5.015$ MeV. The laboratory energy is E_{lab} / nucleon = 84 MeV.

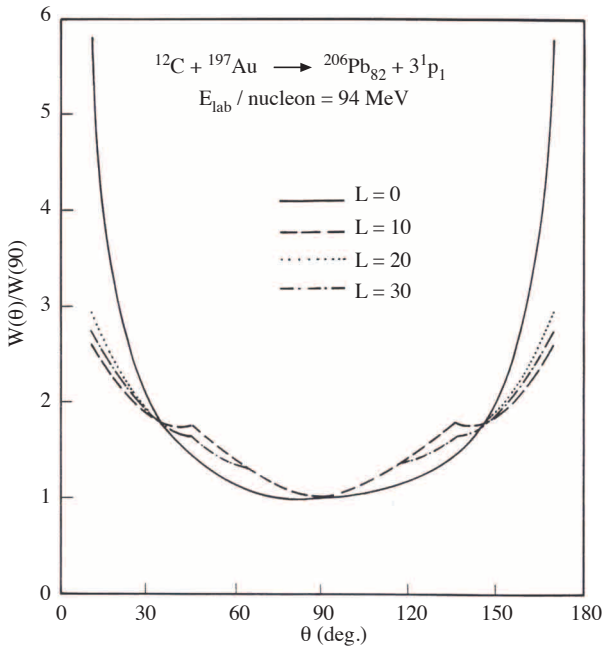

Figure 9. Angular distributions of the fission fragments from the $^{12}\mathrm{C}+\ ^{197}\mathrm{Au} \rightarrow ^{206}\mathrm{pb}_{82}\ + 3\ ^{1}\mathrm{P}_{1}$ reaction at different values of the angular momentum. The nuclear temperature has a value $T = 5.814$ MeV. The laboratory energy is E_{lab} / nucleon = 94 MeV.

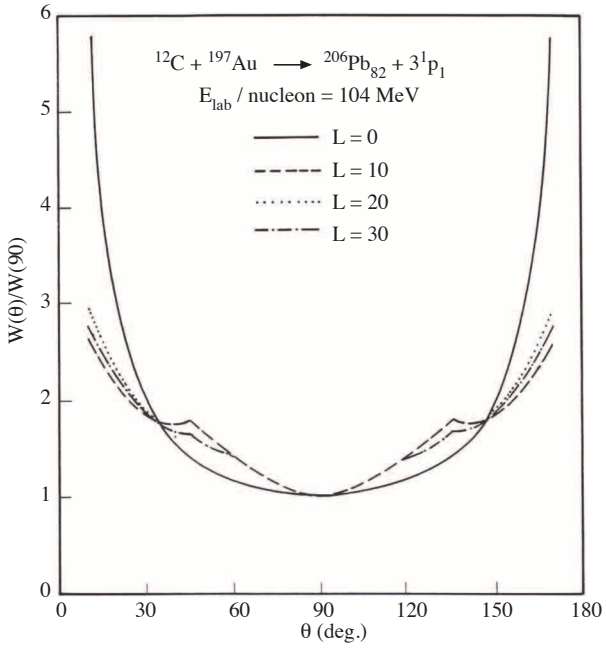

Figure 10. Angular distributions of the fission fragments from the $^{12}\mathrm{C}+\ ^{197}\mathrm{Au} \rightarrow ^{206}\mathrm{pb}_{82}\ + 3\ ^{1}\mathrm{P}_{1}$ reaction at different values of the angular momentum. The nuclear temperature has a value $T = 6.176$ MeV. The laboratory energy is E_{lab} / nucleon = 104 MeV.

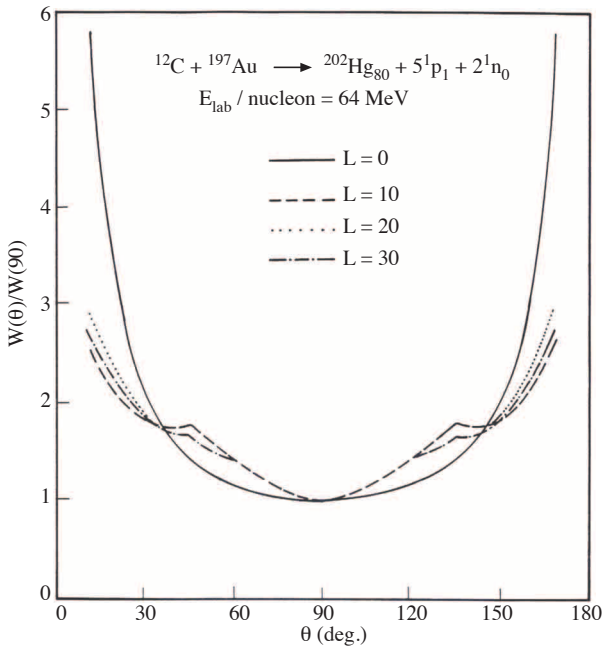

Figure 11. Angular distributions of the fission fragments from the $^{12}C + ^{197}Au \rightarrow ^{202}Hg_{80} + 5\ ^1P^1_{1+2}n_0$ reaction at different values of the angular momentum. The nuclear temperature has a value $T = 4.452$ MeV. The laboratory energy is E_{lab} / nucleon = 64 MeV.

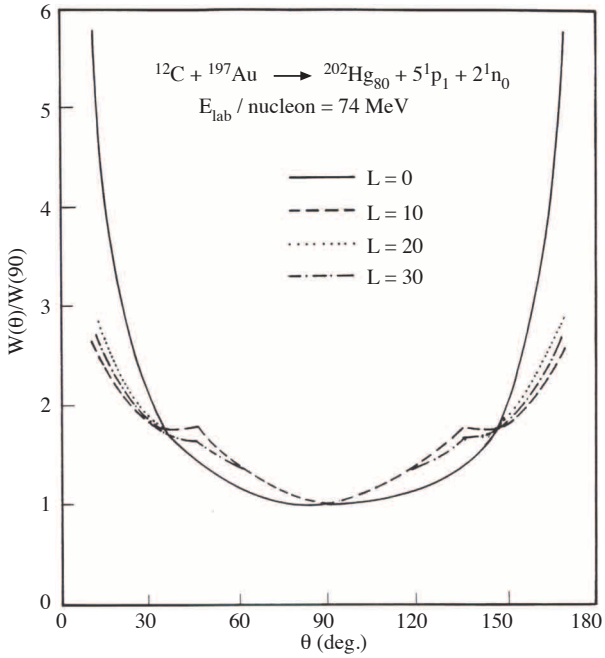

Figure 12. Angular distributions of the fission fragments from the $^{12}C + ^{197}Au \rightarrow ^{202}Hg_{80} + 5\ ^1P^1_{1+2}n_0$ reaction at different values of the angular momentum. The nuclear temperature has a value $T = 4.914$ MeV. The laboratory energy is E_{lab} / nucleon = 74 MeV.

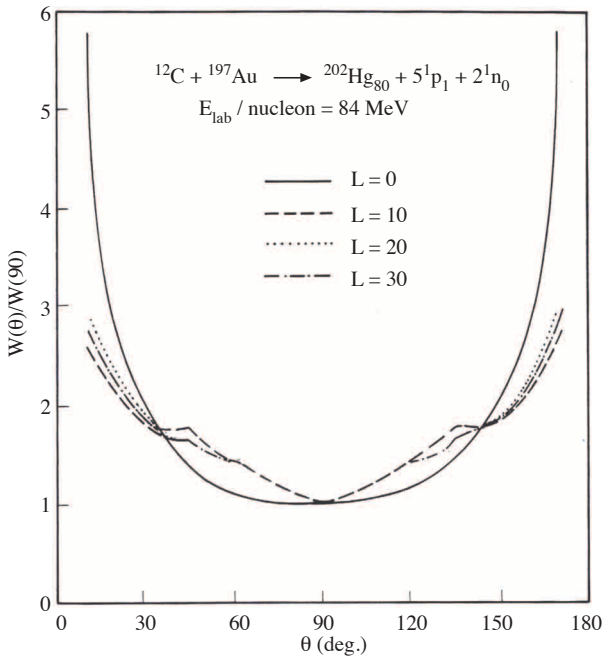

Figure 13. Angular distributions of the fission fragments from the $^{12}C + ^{197}Au \rightarrow ^{202}Hg_{80} + 5\ ^1P^1_{1+2}n_0$ reaction at different values of the angular momentum. The nuclear temperature has a value $T = 5.337$ MeV. The laboratory energy is E_{lab} / nucleon = 84 MeV.

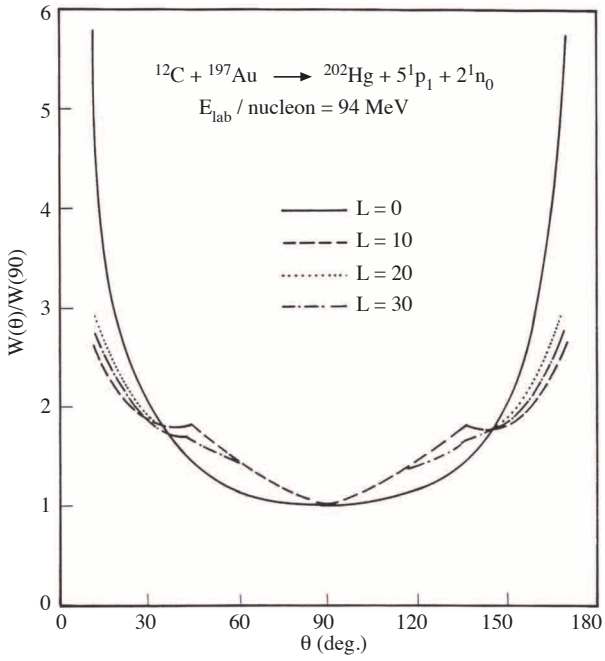

Figure 14. Angular distributions of the fission fragments from the $^{12}C + ^{197}Au \rightarrow ^{202}Hg_{80} + 5\ ^1P^1_{1+2}n_0$ reaction at different values of the angular momentum. The nuclear temperature has a value $T = 5.728$ MeV. The laboratory energy is E_{lab} / nucleon = 94 MeV.

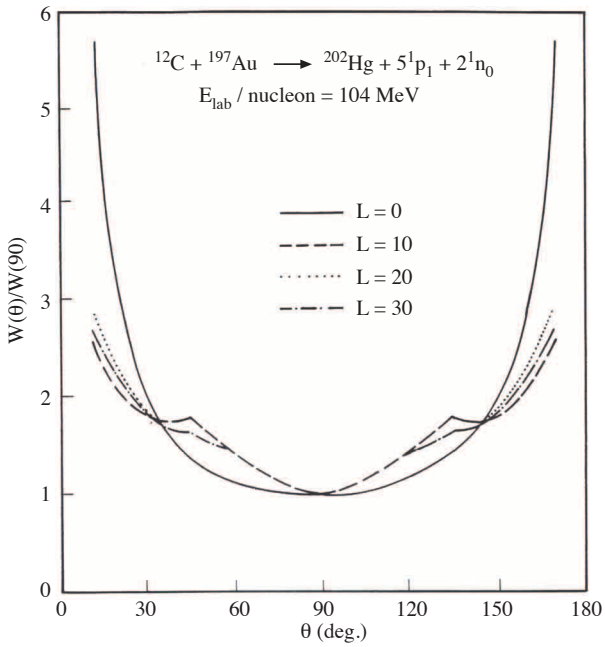

Figure 15. Angular distributions of the fission fragments from the $^{12}\mathrm{C} + {}^{197}\mathrm{Au} \rightarrow {}^{202}\mathrm{Hg}_{80} + 5\ {}^{1}\mathrm{P}^{1}_{1+2}\,\mathrm{n}_0$ reaction at different values of the angular momentum. The nuclear temperature has a value $T = 6.094$ MeV. The laboratory energy is E_{lab} / nucleon = 104 MeV.

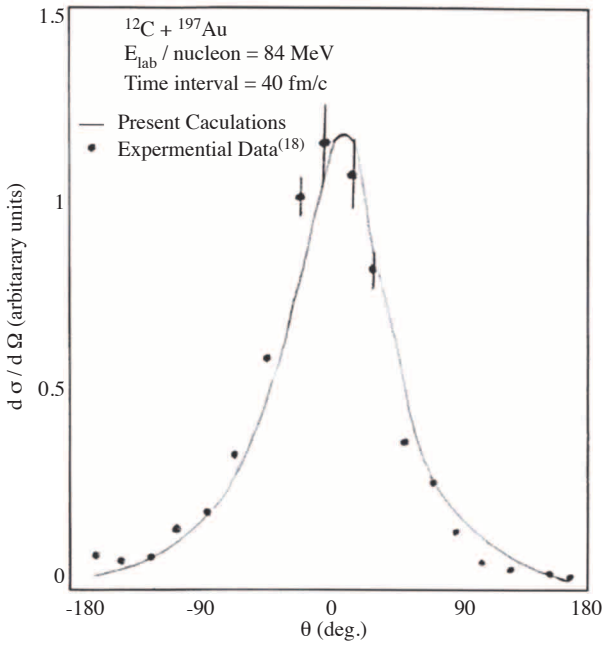

Figure 16. Angular distributions of the emitted protons as function of time, for time interval of 40 fm/c. Positive angels correspond to positive momentum transfer component of the impact parameter of the emitted particles. The solid curves stand for the present theoretical calculations. The dots are the experimental data from reference [18].

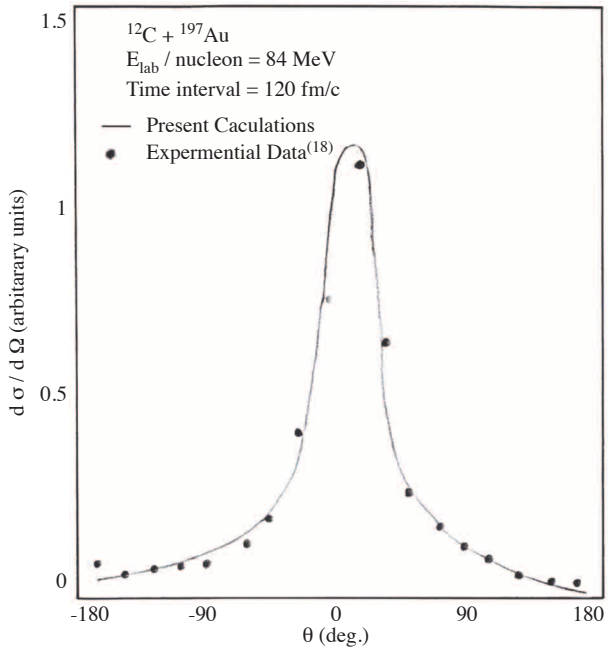

Figure 17. Angular distributions of the emitted protons as function of time, for time interval of 120 fm/c. Positive angels correspond to positive momentum transfer component of the impact parameter of the emitted particles. The solid curves stand for the present theoretical calculations. The dots are the experimental data from reference [18].

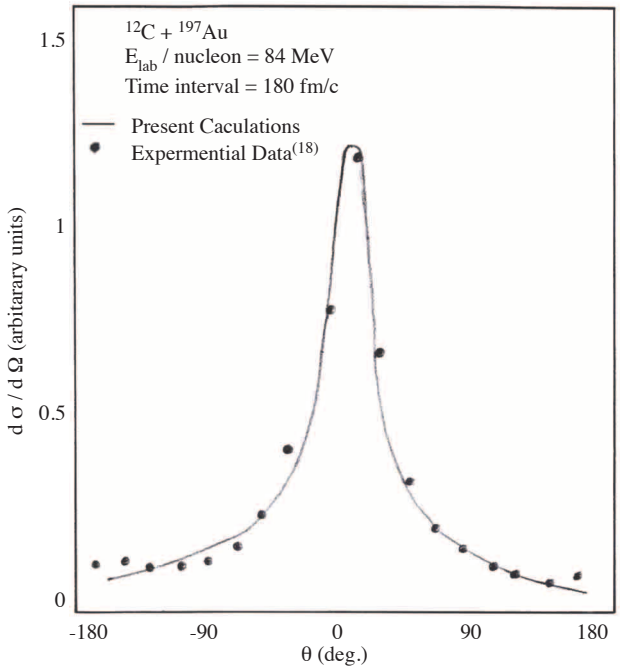

Figure 18. Angular distributions of the emitted protons as function of time, for time interval of 180 fm/c. Positive angels correspond to positive momentum transfer component of the impact parameter of the emitted particles. The solid curves stand for the present theoretical calculations. The dots are the experimental data from reference [18].

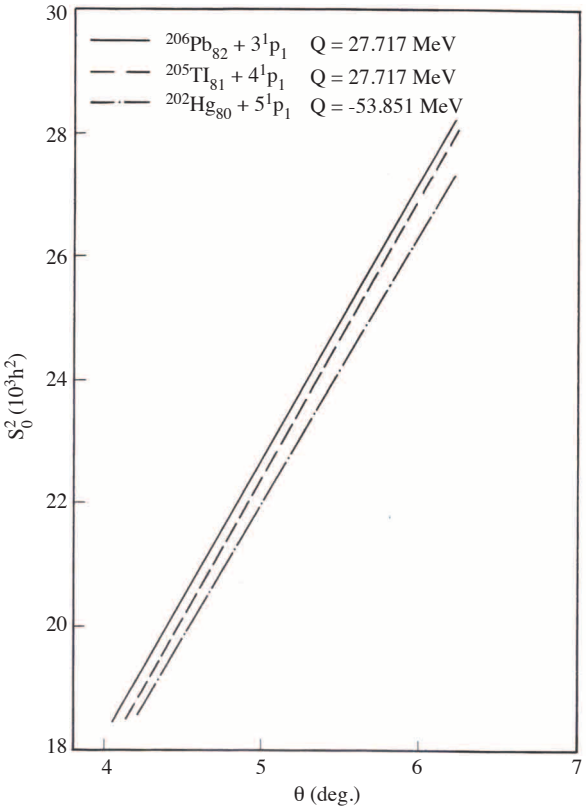

Figure 19. The variances of the fission fragments and their dependence on the nuclear temperature.

In Figure (1), the angular distributions of the ratio $W(\theta)/W(90)$ are shown at incident energy 64 MeV per nucleon for different values of the total angular momentum for outgoing reaction products $^{205}\mathrm{T1} + 4^1\mathrm{P}$. From the Figure (1), we see that the ratios $W(\theta)/W(90)$ are symmetric around the angel $\theta = 90$. Also, the ratio $W(\theta)/W(90)$ in the angular range from $\theta = 10$–30° decreases as L increases and the most greater value is obtained for L = 0, while the most smaller value for $W(\theta)/W(90)$ is obtained for $L = 10$. We notice also that $W(\theta)/W(90)$ in the angular range $\theta = 30$–60° decreases as L increases and that ratios $W(\theta)/W(90)$ are identical for the cases of angular momenta with L =20, $L = 30$. In this region, the ratio $W(\theta)/W(90)$ is the smallest value for $L = 0$, while the greatest value is obtained for $L = 10$. In the angular range $\theta = 60$–90°, the calculated ratios $W(\theta)/W(90)$ for the cases of angular momenta with values $L = 10$, $L = 20$, $L = 30$ are the same and $W(\theta)/W(90)$ for $L = 0$ is the smaller than the three others for $L = 10, 20, 30$. At the angel $\theta = 90^\circ$, all the calculated values of the ratio $W(\theta)/W(90)$ are identical for all values of angular momenta with values $L = 10$, $L = 20$, $L = 30$.

Figures (2)–(5) show the present calculations of the ratios $W(\theta)/W(90)$ for different values of the incident energies per nucleons at 74, 84, 94 and 104 MeV, showing the same behavior as that described in Figure (1). Numerical calculations are also carried out for the other two types of reaction products types of reaction products where for the reaction products type $^{206}\mathrm{pb}_{82} + 3\ ^1\mathrm{P}_1$ the calculations are shown in Figures (6)–(10), while for the case of reaction products type $^{202}\mathrm{Hg}_{80} + 5\ ^1\mathrm{P}_1 + 2\ ^1\mathrm{n}_0$ the calculations are given in Figures (11)–(15).

The angular distributions of the emitted particles as a function of the emission time are shown in Figures (16)–(18), for different values of time intervals. The positive angels correspond to positive momentum transfer component respect to the direction of the impact parameter. Most of the emitted particles come from the hot excited subsystem.

The calculated values of the variances S_0^2 as a function of the nuclear temperature are shown in Figure (19) for the three reaction products type $^{205}\mathrm{T1}_{81}+4\,^1\mathrm{P}_1$, $^{206}\mathrm{Pb}_{82}+3\,^1\mathrm{P}_1$ and $^{202}\mathrm{Hg}_{80}+5\ ^1\mathrm{P}_1+2\ ^1\mathrm{n}_0$.

The Q-values for these reactions are -34.470 MeV, -27.717 MeV and -53.851 MeV, respectively. Also, the obtained results of the calculated values of the variances for the different reaction products, incident energies and temperatures T are listed in Table 1.

Table 1. Calculated values of the variances.

Reaction Products	G (MeV)	E_{lab} (MeV)	T (MeV)	S_0^2 (MeV)
$^{206}\mathrm{pb}_{82}$ + 3 $^1\mathrm{P}_1$	−27.717	64	4.060	18.394
		74	4.563	20.668
		84	5.015	22.716
		94	5.814	26.337
		104	6.176	27.973
$^{205}\mathrm{T1}_{81}$ + 4 $^1\mathrm{P}_1$	−34.470	64	4.029	18.104
		74	4.534	20.376
		84	4.989	22.419
		94	5.406	24.291
		104	5.792	26.028
$^{202}\mathrm{Hg}_{80}$ + 5 $^1\mathrm{P}_1$ + 2 $^1\mathrm{n}_0$	−53.851	64	4.452	19.527
		74	4.914	21.555
		84	5.337	23.407
		94	5.728	25.124
		104	6.094	26.730

5. Discussion and conclusion

In the present work, the statistical scission model is used in studying fission process from heavy ion interactions. We considered the case of $^{12}\mathrm{C}$ interacting with $^{197}\mathrm{Au}$ target leading to fission products of a deformed nucleus and few nucleons. The angular distributions of the fission fragments have been numerically calculated for different incident energies and nuclear temperatures.

The angular distributions as shown in Figures (1)–(15) are strongly dependent on the nuclear temperature showing symmetric shapes around $\theta = 90^\circ$. Figures (16)–(18) show good agreement between the present theoretical calculations of the emitted particles distributions (solid curves) to those with experimental proton cross-sections. Also, the calculated variances are temperature dependent. The present calculations are in good agreements with heavy ion induced fission [15] calculations and with multifragmentation [16, 17] calculations.

Therefore, we conclude that the heavy ion induced fission, leading to a deformed nucleus with few nucleons, are well described using the statistical scission model. The present calculations show that the angular

distributions and the variances are strongly dependent on the nuclear temperature, which means that it should be included in any calculations.

References

[1] H. Rossner, J. R. Huizenga and W. U. Schroder, *Phys. Rev.*, **C33**, (1986), 560.

[2] B. B. Back, H. G. Clerc, R. R. Betts, B. G. Glagola and B. D. Wilkins, *Phys. Rev. Letters*, **46**, (1981), 1068.

[3] H. Rossner, D. Hilscher, E. Holub, G. Ingold, U. Jahnke, H. Orf, J. R. Huizenga, J. R. Birkelund, W. U. Schroder and W. W. Wilcke, *Phys. Rev.*, **C27**, (1983), 2666.

[4] M. B. Tsang, H. Utsunomiya, C. K. Gelbke, W. G. Lynch, B. B. Back, S. Saini, P. A. Baisden and M. A. McMahan, *Phys. Letters*, **B 129**, (1983), 18.

[5] B. B. Back, R. R. Betts, K. Cassidy, B. G. Glagola, J. E. Gindler, L. E. Glendenin and B. D. Wilkins, *Phys. Rev. Letters*, **50**, (1983), 818.

[6] K. T. Lesko, S. Gil, A. Lazzarini, V. Melag, A. G. Seamster and R. Vandenbosch, *Phys. Rev.*, **C27**, (1983), 2999.

[7] M. B. Tsang, D. Ardouin, C. K. Gelbke, W. G. Lynch and Z. R. Xu, *Phys. Rev.*, **C28**, (1983), 747.

[8] A. Gavron, P. Eskola, A. J. Sierk, J. Boissevain, H. C. Britt, K. Eskola, M. M. Fowler, H. Ohm, J. B. Wilhelmy, C. Wald and R. L. Ferguson, *Phys. Rev. Letters*, **52**, (1984), 589.

[9] M. Prakash, V. S. Ramamurthy, S. S. Kapoor and J. M. Alexander, *Phys. Rev. Letters*, **52**, (1984), 990.

[10] S. Cohen, F. Plasil and W. J. Swiatecki, *Ann. Phys. (N. Y.)*, **82**, (1974), 557.

[11] T. Ericson, *Adv. Phys.*, **9**, (1960), 9.

[12] T. Dossing and N. Bohr, *Phys. Lett.*, **54**, (1985), 1596.

[13] P. D. Bond, *Phys. Rev.*, **C32**, (1985), 471.

[14] P. D. Bond, *Phys. Rev.*, **C32**, (1985), 483.

[15] A. Osman and M. Y. H. Farag, *I1 Nuovo Cimento*, **108A**, (1995), 155.

[16] A. Osman and M. Y. H. Farag, *I1 Nuovo Cimento*, **109A**, (1996), 1449.

[17] A. Osman and M. Y. H. Farag, *Heavy Ion Physics*, **10**, (1999), 73.

[18] J. Aichelin, *Phys. Rev.*, **33**, (1986), 537.